Further studies on the physics potential of an experiment using LHC neutrinos

OPEN ACCESS
IOP Publishing
Journal of Physics G: Nuclear and Particle Physics
J. Phys. G: Nucl. Part. Phys. **47** (2020) 125004 (18pp)
https://doi.org/10.1088/1361-6471/aba7ad

Further studies on the physics potential of an experiment using LHC neutrinos

N Beni[1,2], M Brucoli[2], V Cafaro[3], T Camporesi[2], F Cerutti[2], G M Dallavalle[3,*], S Danzeca[2], A De Roeck[2], A De Rújula[4], D Fasanella[2], V Giordano[3], C Guandalini[3], A Ioannisyan[2,5], D Lazic[6], A Margotti[3], S Lo Meo[3,7], F L Navarria[3], L Patrizii[3], T Rovelli[3], M Sabaté-Gilarte[2,8], F Sanchez Galan[2], P Santos Diaz[2], G Sirri[3], Z Szillasi[1,2] and C-E Wulz[9]

[1] Hungarian Academy of Sciences, Inst. for Nuclear Research (ATOMKI), Debrecen, Hungary
[2] CERN, CH-1211 Geneva 23, Switzerland
[3] INFN sezione di Bologna and Dipartimento di Fisica dell' Università, Bologna, Italy
[4] Inst. de Estructura de la Materia, Consejo Superior de Investigaciones Cientificas (CSIC), Madrid, Spain
[5] A.Alikhanyan National Science Laboratory, Yerevan Physics Institute, Yerevan, Armenia
[6] Boston University, Department of Physics, Boston, MA 02215, United States of America
[7] ENEA Research Centre E. Clementel, Bologna, Italy
[8] Universidad de Sevilla, Spain
[9] Institute of High Energy Physics of the Austrian Academy of Sciences, and Vienna University of Technology, Vienna, Austria

E-mail: Marco.Dallavalle@cern.ch

Received 20 April 2020, revised 8 July 2020
Accepted for publication 20 July 2020
Published 4 November 2020

Abstract

We discuss an experiment to investigate neutrino physics at the LHC, with emphasis on tau flavour. As described in our previous paper Beni *et al* (2019 *J. Phys. G: Nucl. Part. Phys.* **46** 115008), the detector can be installed in the decommissioned TI18 tunnel, ≈480 m downstream the ATLAS cavern, after the first bending dipoles of the LHC arc. The detector intercepts the intense

*Author to whom any correspondence should be addressed.

neutrino flux, generated by the LHC beams colliding in IP1, at large pseudorapidity η, where neutrino energies can exceed a TeV. This paper focuses on exploring the neutrino pseudorapity versus energy phase space available in TI18 in order to optimize the detector location and acceptance for neutrinos originating at the pp interaction point, in contrast to neutrinos from pion and kaon decays. The studies are based on the comparison of simulated pp collisions at $\sqrt{s} = 13$ TeV: PYTHIA events of heavy quark (c and b) production, compared to DPMJET minimum bias events (including charm) with produced particles traced through realistic LHC optics with FLUKA. Our studies favour a configuration where the detector is positioned off the beam axis, slightly above the ideal prolongation of the LHC beam from the straight section, covering $7.4 < \eta < 9.2$. In this configuration, the flux at high energies (0.5–1.5 TeV and beyond) is found to be dominated by neutrinos originating directly from IP1, mostly from charm decays, of which ≈50% are electron neutrinos and ≈5% are tau neutrinos. The contribution of pion and kaon decays to the muon neutrino flux is found small at those high energies. With 150 fb^{-1} of delivered LHC luminosity in Run 3 the experiment can record a few thousand very high energy neutrino charged current (CC) interactions and over 50 tau neutrino CC events. These events provide useful information in view of a high statistics experiment at HL–LHC. The electron and muon neutrino samples can extend the knowledge of the charm PDF to a new region of x, which is dominated by theory uncertainties. The tau neutrino sample can provide first experience on reconstruction of tau neutrino events in a very boosted regime.

Keywords: LHC neutrinos, TeV neutrinos, neutrino experiment at LHC, LHC forward physics

(Some figures may appear in colour only in the online journal)

1. Introduction

Intense fluxes of neutrinos of all flavours are produced in collisions of the LHC proton beams at the IP1 and IP5 interaction points, respectively hosting the ATLAS and CMS detectors. At large pseudorapidity η, neutrinos attain TeV energies, a new domain much beyond the energy of available neutrino data from laboratory experiments [1, 2]. At very high energy, astrophysical measurements exist [3], with limited amounts of data.

Tau flavour neutrinos are especially interesting, since there are hints of deviations from the standard model in the third generation, in the measurement of the W decay branching ratio to τ at LEP [4] and in measurements of the semileptonic decays of B to D and D^* [5].

In a previous paper we investigated the feasibility of a neutrino experiment at the LHC [1]. We focussed on high energy neutrinos in two η ranges (figure 1):

- $4 < \eta < 5$: high energy neutrinos are produced in leptonic W decays; about 33% tau neutrinos
- $6.5 < \eta < 9.5$: neutrinos from c and b decays; about 5% tau neutrinos, mostly from D_s decays.

Four potential sites were identified and studied on the basis of (a) expectations for neutrino interaction rates, flavour composition and energy spectrum, (b) predicted backgrounds and in-situ measurements, performed with a nuclear emulsion detector and radiation monitors. One

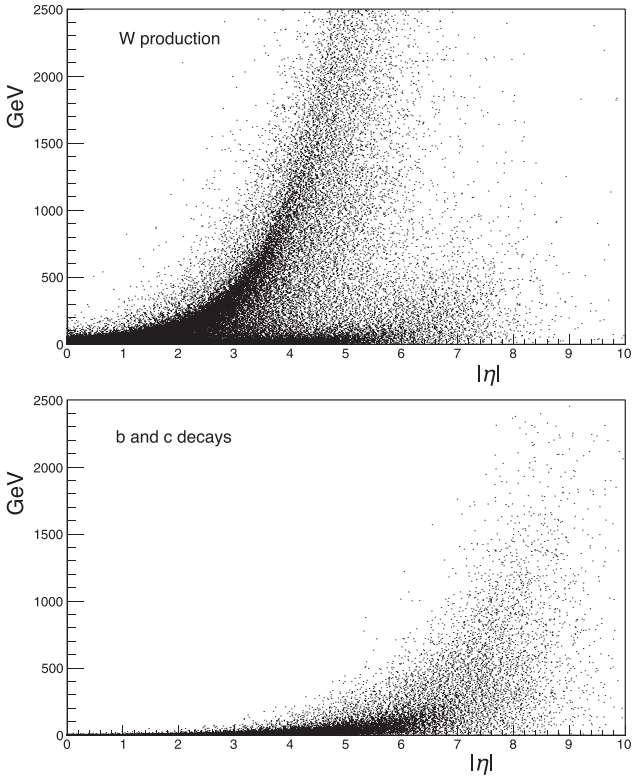

Figure 1. Scatter plots of neutrino energy versus pseudorapidity η in pp collision events [1]. Events generated with PYTHIA [6]. Top: neutrinos from leptonic and hadronic W decays. Bottom: neutrinos from b and c decays.

of the locations appeared to qualify for hosting a neutrino experiment. It lies at 480 m from the ATLAS IP1, where the cavern of the TI18 tunnel intercepts the prolongation of the beam axis, after the beginning of the LHC arc. That tunnel, now in disuse, was employed to inject electron beams in LEP. A small mass detector located there can observe neutrinos from the IP within polar angles < 2.5 mrad ($\eta > 6.7$). A similar tunnel (TI12) exists at the opposite end of ATLAS. No such tunnels are present near the CMS IP.

In this paper we investigate the neutrino phase space in the energy-η plane available to an experiment located in TI18. Focus is on characteristics of the neutrino flux within acceptance, separating neutrinos produced during pp collisions and those originating later in pion and kaon decays.

The experimental constraints are described in section 2. We assume that the detector is totally passive, made of emulsions and lead absorbers, as used for our tests [1]. However, the presented arguments apply to any detectors with similar mass and acceptance. The neutrino flux composition and occupancy in energy versus η is studied in section 3. Simulations are performed using PYTHIA (version 8.226) [6] and the LHC FLUKA package of CERN EN-STI [7–11], with embedded LHC optics. It is shown that a detector acceptance in $7.4 < \eta < 9.2$, i.e. slightly off the prolongation of the beam axis from IP1, favours neutrinos from charm decays, and in particular tau neutrinos. In section 3, energy distributions and rates of neutrino events are compared for two detectors with acceptance in $7.4 < \eta < 8.1$ and $8.0 < \eta < 9.2$, and an LHC luminosity of 150 fb^{-1}. Event rate expectations are calculated by neutrino flavour

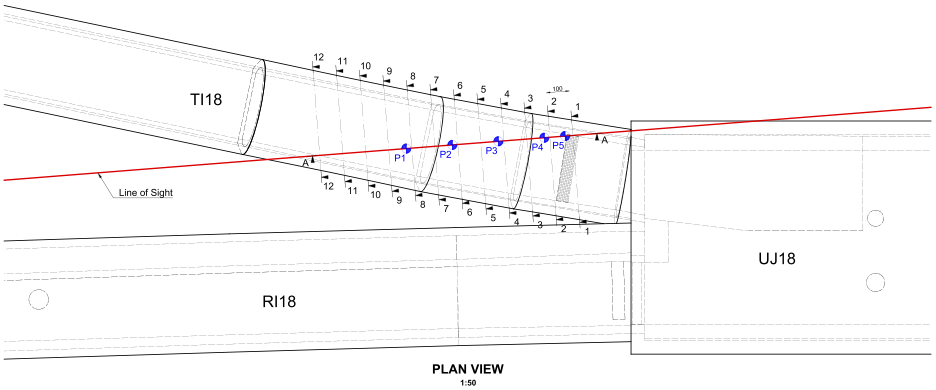

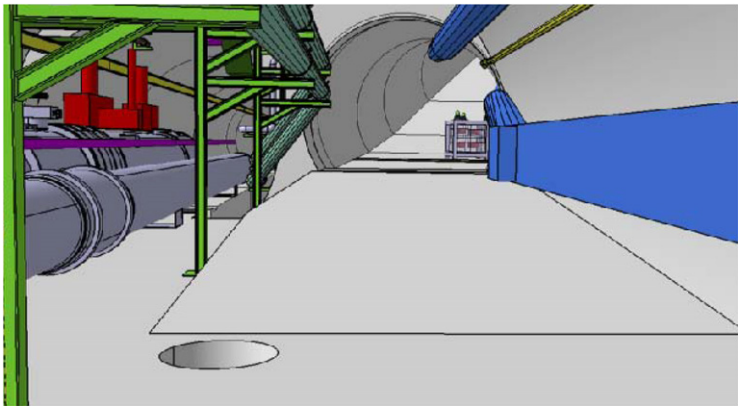

Figure 2. TI18 tunnel at the connection with the LHC tunnel [12]. Top: planar view; IP1 is 480 m on the left; in red the beam LoS from IP1; survey marks (floor heights (*P*) along the LoS and tunnel contours at different heights) are also shown. Bottom: 3d view.

and take into account only the detector mass; matters related to neutrino identification are detector specific and are not discussed.

2. Experiment generalities

A first requirement for the experiment feasibility is a location in which particles coming directly from the IP are screened off, except for muons and neutrinos, by rock, or by the absorbers that protect experimental areas and LHC components. A second requirement is that the local backgrounds from secondary interactions in collimators, beam pipe and other machine elements are low. Intensity and composition of these machine induced backgrounds vary rapidly along the LHC. Specifically for a detector located in the TI18 tunnel (figure 2), energetic charged particles are deviated by the LHC arc optics and do not reach the detector, and the beam line-of-sight (LoS) from IP1 traverses about 100 m of rock before crossing the TI18 cavern. However, the useful space is restricted in length to a few metres and the floor is on a slope that lies higher than the LoS from a minimum of 5 cm growing in steps up to 50 cm: these are limitations for a standard massive neutrino detector, but not in this case, as shown in the following.

The νN cross section grows rapidly with the neutrino energy, linearly from 10 GeV to a few hundred GeV [2]. Therefore, if this trend continues, at high energy the detector can be light, featuring a mass of a few tons, and still collect a considerable sample of neutrino interactions

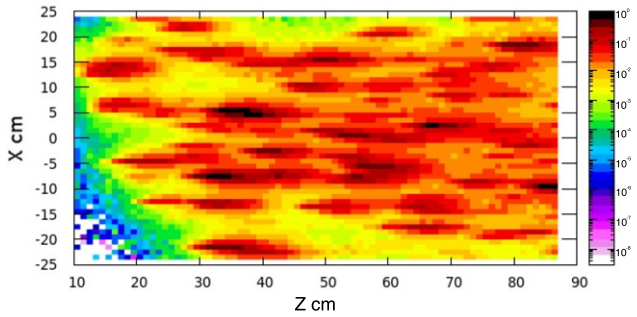

Figure 3. FLUKA [7, 8] simulation of hundred electron ν, with $0.2 < E < 1.2$ TeV, interacting in a 77 cm deep structure of OPERA-like lead-emulsion layers. Incoming neutrinos are randomly distributed over an area X, Y of 50×30 cm^2. Normalization is to the elementary volume with the largest energy deposit.

[1]; the energy spectrum of the observed events will be hard, because the higher energy neutrinos have larger interaction cross sections. If lead is used as target, the detector becomes very compact: 1 ton of lead is a block of 1 m length and 30×30 cm^2 cross section.

Most neutrino experiments designed for tagging tau neutrino interactions embedded nuclear emulsions in their detectors [13–15]. Emulsions are efficient for reconstructing the vertex of tau decays. The OPERA experiment [13] used a modular design: emulsions interleaved with thin layers of lead, packed together into a 'brick'. An OPERA brick is 128 mm wide, 104 mm high, and 78 mm thick, with 56 mm lead; it weighs 8.3 kg. A 1 ton detector requires 120 such bricks.

Thus for the sake of the present studies, we will assume detectors consisting of lead-emulsion layers subdivided in OPERA-like bricks.

Emulsion layers in an OPERA brick are uniformly spaced: a one millimeter lead sheet separates two consecutive layers, for a total of 56 layers. The brick thickness is short for reconstructing with high efficiency a decay vertex of a tau with TeV energy. The expected decay length of a TeV tau lepton is a few centimeters, much longer than in the OPERA case, suggesting that the structure should be extended to include at least 200 layers, i.e. at least $\approx$4 bricks thick. Besides, a TeV electron shower has a 95% energy containment length of 22 cm, about 4 OPERA bricks. Figure 3, shows hundred charged current (CC) interactions of electron neutrinos with energies from 0.2 to 1.2 TeV, simulated with FLUKA [7, 8] in a structure like an OPERA brick but repeated ten times in depth (Z), X being the orthogonal coordinate in the horizontal plane, and Y the vertical coordinate.

The emulsion stacks are very good for reconstructing the vertex of a neutrino interaction, but they cannot easily provide a measurement of the neutrino energy. On an event by event basis the neutrino energy can be estimated using the methods developed in OPERA and other emulsion based detectors, which for instance exploit the correlation between track multiplicity and neutrino energy [16–18]. The achievable resolution depends on the brick structure; a resolution of 50% in the 0.1–1 TeV energy range seems realistic. However, also kinematics can be exploited: in the regime of longitudinal momentum p_{L} much larger than transverse momentum p_{T}, the pseudorapidity of particles emerging from the IP is proportional to the logarithm of the energy, a relation smeared by the particle p_{T} distribution. Different η ranges have different average energy, as seen in figure 4. The $\log(E_\nu)$ versus η linear dependence can also be useful for defining a fiducial phase space so to reject obvious outliers.

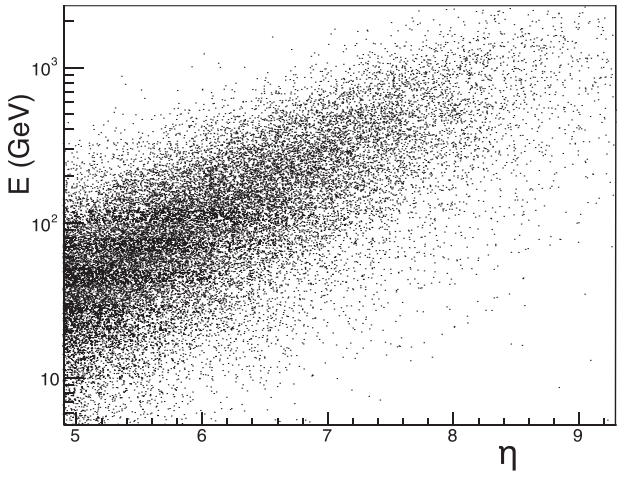

Figure 4. A scatter plot of log (E) versus η for neutrinos from b and c quark decays. Events generated with PYTHIA [6].

Therefore, in the following studies we consider two detectors made of OPERA-like bricks, of ≈1 ton each, ≈1 m in length (i.e. at least 12 brick thick). They cover different η ranges, to be optimised for high energy and tau flavour neutrinos. We do not aim for high resolution in energy, but rather for having two independent energy bins, one for each detector.

Aside, we remark that the track extrapolation between emulsions across a lead layer becomes more complex when the track density is high; a level of 10^5 tracks/cm^2 is regarded as a good condition. Thus, given the background estimates in TI18 [1], it is essential that emulsion exposure does not exceed 30 fb^{-1}. In view of the luminosity that LHC is expected to deliver in 2022–2024 (Run 3), it means replacement of the bricks a few times per year. Then, extrapolating to HL–LHC, conditions will be prohibitive and different detector technologies should be envisaged. However the arguments exposed in this paper apply to any detector with similar mass and η acceptance.

3. Neutrino flux

We aim at exploring the neutrino pseudorapity versus energy phase space available in TI18 in order to optimize the detector location and acceptance for neutrinos originating at the pp interaction point, in contrast to neutrinos from pion and kaon decays, with emphasis on tau neutrinos. The studies are based on the comparison of simulated proton–proton collisions at $\sqrt{s} = 13$ TeV: PYTHIA [6] events of heavy quark (c and b) production, against DPMJET [9, 10] minimum bias events with produced particles traced through LHC optics with FLUKA [7, 8, 11]. DPMJET comprises charm production [19].

PYTHIA was used in our previous paper [1] to estimate the neutrino flux in TI18 for $\eta > 6.7$. At high energy most of the flux originates from c (≈92%) and b (≈8%) decays; about 5% of the neutrinos are of the tau flavour, originating in $D_s \to \tau\nu_\tau$ decays and in the subsequent τ decays. Neutrinos from pion decays pointing towards TI18 are predicted to have mostly low energies. The $\gamma c\tau$ of a pion exceeds 500 m already at 10 GeV, and it reaches 5 km at 100 GeV. Therefore most high energy pions are deviated by the LHC optics and interact in the LHC beam pipe or in the rock before they can decay. Neutrinos from kaon decays pointing towards

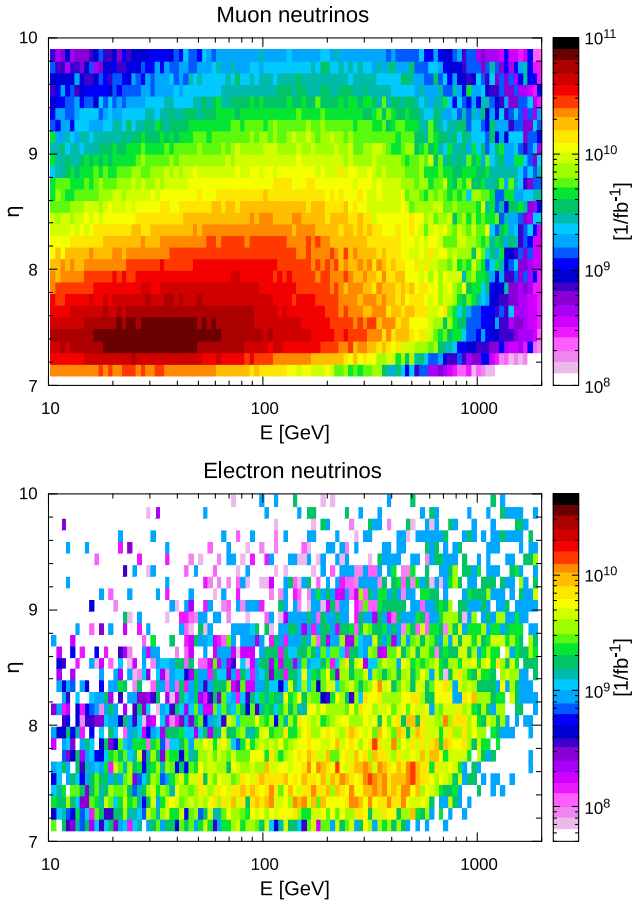

Figure 5. Scatter plots of neutrino pseudorapidity η versus energy. Events generated by using DPMJET event generator; both pion/kaon decays and charm production were activated. Produced particles are traced through LHC optics with FLUKA. Top: muon neutrinos. Bottom: electron neutrinos.

TI18 can have higher energies, since the $\gamma c\tau$ for a 100 GeV kaon is about 740 m, however the kaon/pion production rate ratio is only about 11%.

The underlying theoretical uncertainties in the very large rapidity region are big. PYTHIA was tested in depth by the LHC experiments; it reproduces the features of proton–proton interactions with good accuracy. Measurements of charged particle production in the forward direction were performed by LHCb [20] in the pseudorapidity range $2.0 < \eta < 4.5$, and by TOTEM [21] in $5.3 < \eta < 6.5$, and found in reasonable agreement with PYTHIA expectations. However, no experimental crosschecks exist for the very forward η range that our detector subtends.

We use PYTHIA 8.226 with its default tune for charm and bottom quark production in proton–proton collisions [6, 22]. Previous calculations of neutrino flux and CC event rates for a far forward experiment were performed by De Rùjula, Fernandez and Gòmez-Cadenas [23] (1993). They made an analytical calculation using two variants of a non-perturbative QCD model (quark gluon string model), which had large uncertainties in predicting the transverse momentum distribution for the produced hadrons. A recent paper by Bai *et al* [24] has

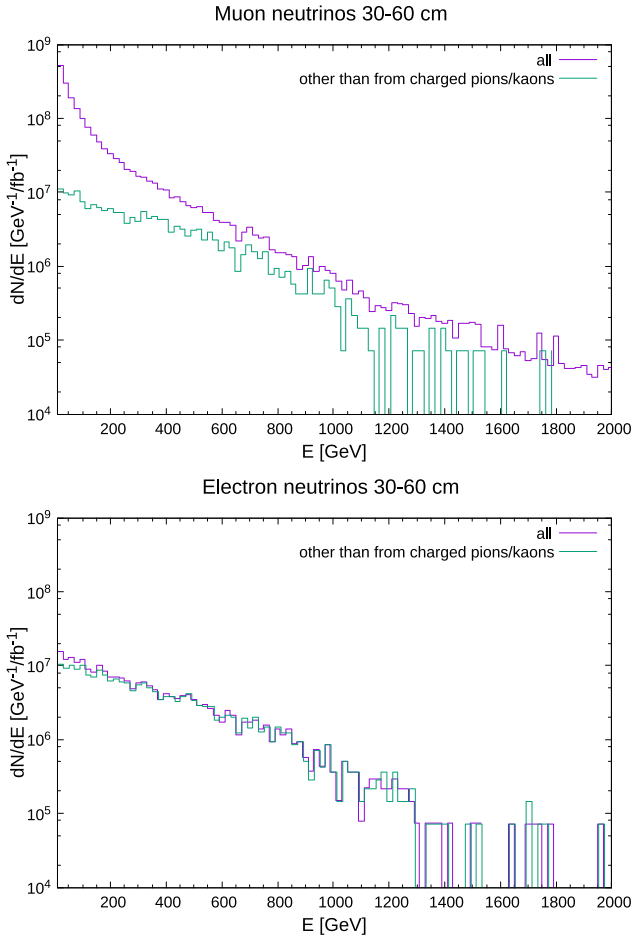

Figure 6. Predicted fluxes of neutrinos for the radial distance $30 < R < 60$ cm from the beam axis in TI18 ($7.4 < \eta < 8.1$) from DPMJET with produced particles traced through LHC optics with FLUKA. Top: muon neutrinos. Bottom: electron neutrinos.

made a full theoretical calculation of neutrino rates and energy spectra in the far forward region, including pion and kaon decays, and explored the uncertainties. The calculation is state-of-the-art, with next-to-leading order QCD radiative corrections in the production cross-sections and k_{T}-smearing of the parton distribution functions. The expected neutrino flux from heavy quark decays for $\eta > 6.87$ and an LHC luminosity of 3000 fb^{-1} is similar to our results using PYTHIA in [1]. Unfortunately, we cannot use their results for off-beam-axis configurations as they are not expressed as a double differential in neutrino pseudorapidity and energy.

Park [25] (2011) used a PYTHIA generator version 6 with parameter set tuned to Tevatron data and very early LHC data, and a lower D_s production cross section. The calculation included a crude simulation of the LHC optics and an estimate of the contribution of neutrinos from pion and kaon decays. The detector was assumed to be on the beam LoS, and the calculation shows a peak for low energy muon neutrinos very close to the beam axis ($\eta > 9$). A thorough simulation study of the expected flux in TI18 very close to the beam LoS (within 10 cm around it, i.e.

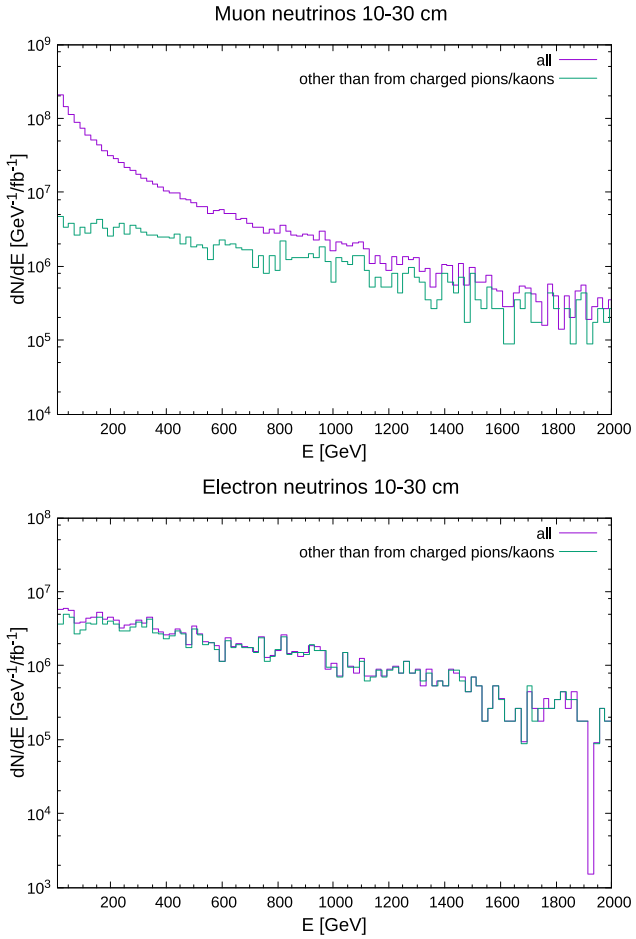

Figure 7. Predicted fluxes of neutrinos for the radial distance $10 < R < 30$ cm from the beam axis in TI18 ($8.0 < \eta < 9.2$) from DPMJET with produced particles traced through LHC optics with FLUKA. Top: muon neutrinos. Bottom: electron neutrinos.

$\eta > 9.1$) was presented in a recent paper by the FASER collaboration [26], but the calculated energy spectra cannot be simply transposed to a different η range. The exact distribution at about 500 m from the IP critically depends on the transport of the parent pion/kaon along the LHC optics.

The calculations we are reporting were produced by CERN EN-STI group specialized in FLUKA simulations of LHC, in which events were produced by an independent event generator and products tracked through the state-of-the-art LHC optics. Proton–proton collisions were generated with FLUKA using the embedded DPMJET event generator [7–11], which describes particle production in pp minimum-bias events, including charm production; then pions and kaons, before decaying, were transported through LHC elements and environment material up to TI18. Information was stored separately for neutrinos and antineutrinos, and by flavour. Figure 5 shows the predicted fluence in η versus energy, for the pseudorapidity range under consideration, for muon and electron neutrinos, in 1 fb^{-1}. Electron neutrinos show the η vs ln(E) dependence expected for particles from the IP as in figure 4. The distribution falls very

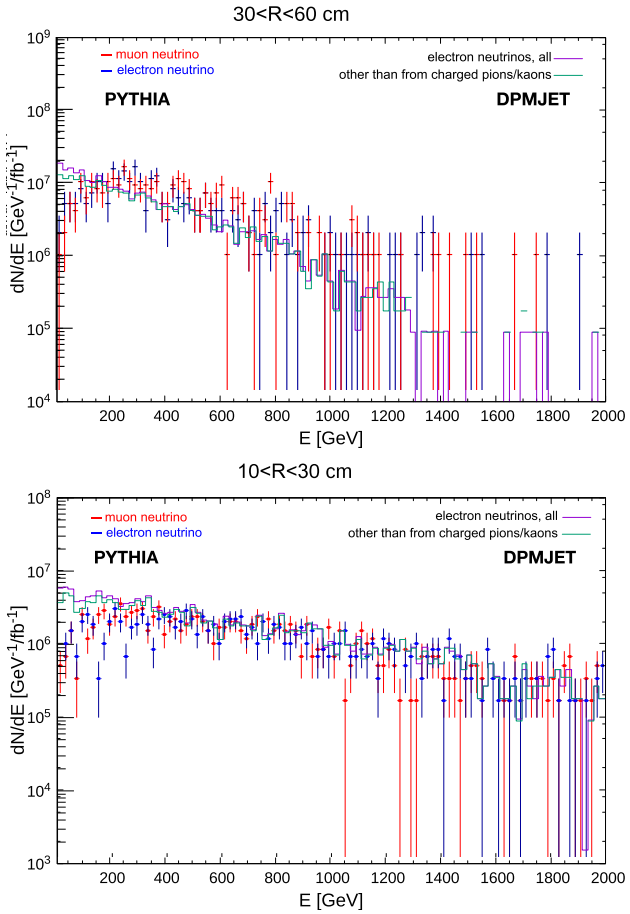

Figure 8. Predicted fluxes of muon and electron neutrinos from heavy quark c and b decays produced by PYTHIA, superimposed on the predictions for electron neutrinos obtained by the DPMJET. Top: at a radial distance $30 < R < 60$ cm from the beam axis in TI18 ($7.4 < \eta < 8.1$). Bottom: at a radial distance $10 < R < 30$ cm from the beam axis in TI18 ($8.0 < \eta < 9.2$).

rapidly at very large η and it becomes inconvenient to move closer to the beam LoS. In the following we split the study in two pseudorapidity regions: $7.4 < \eta < 8.1$, $8.0 < \eta < 9.2$.

In figure 6 neutrino energy distributions are plotted for the radial distance $30 < R < 60$ cm from the beam axis in TI18, corresponding to $7.4 < \eta < 8.1$, separately according to whether neutrinos originated from pion/kaon decays or not. The plots are consistent with the expectations that electron neutrinos and high energy muon neutrinos do not come from pion/kaon decays. In figure 7 the study is repeated for the radial distance $10 < R < 30$ cm from the beam axis in TI18, corresponding to $8.0 < \eta < 9.2$, with similar conclusions. In figure 8 the flux of muon and electron neutrinos from charm production in LHC pp collisions predicted with PYTHIA is also shown, superimposed to the DPMJET ν_e prediction; the absolute normalisation of the calculated flux is in good agreement, and it confirms that most electron neutrinos originate from charm. In addition the agreement between the shapes of the distributions is impressive when considering the different approaches in p_{T} generation between PYTHIA (heavy quark c and b production) and DPMJET (pp minimum bias).

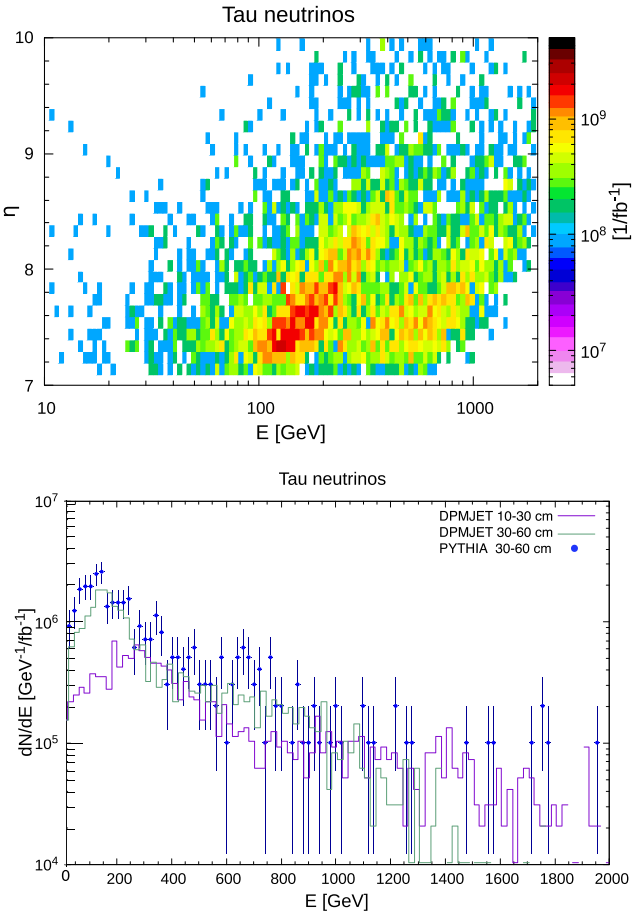

Figure 9. Predicted fluxes of tau neutrinos for the radial distances $10 < R < 30$ cm ($8.0 < \eta < 9.2$) and $30 < R < 60$ cm ($7.4 < \eta < 8.1$) from the beam axis in TI18. Top: scatter plot of tau neutrino pseudorapidity η versus energy. Events generated by using DPMJET event generator; produced particles traced through LHC optics with FLUKA. Bottom: PYTHIA (charm production) tau neutrino energy distribution superimposed to DPMJET.

Tau neutrinos are produced in $D_s \to \tau\nu_\tau$ decays and in the subsequent τ decays. Since the chosen η range has shown high sensitivity to charm decays, we do expect this slightly off-beam-axis configuration to be favourable for tau neutrinos. Figure 9 shows the η versus energy scatter plot and the energy distribution for tau neutrinos in pp collision events generated with DPMJET/FLUKA and with PYTHIA. They confirm the expectations. The flux calculations are normalised to 1 fb^{-1}. Note that the two intensity bands in the η vs $\ln(E)$ scatter plot are predicted from kinematics: neutrinos from D_s decays have little p_T since the mass difference $M_{D_s} - M_\tau$ is small (191 MeV) and they populate the band at lower E; the other band is due to neutrinos from τ decays which do have a larger average p_T ($\approx$592 MeV in three body decays).

In summary, the simulations performed using both PYTHIA and DPMJET agree in showing that a detector acceptance slightly off beam axis, in the $7.4 < \eta < 9.2$ range, is favorable for looking at high energy neutrinos from charm production in pp collisions and consequently for observing tau neutrinos. The state-of-the-art LHC optics emulation with FLUKA shows that

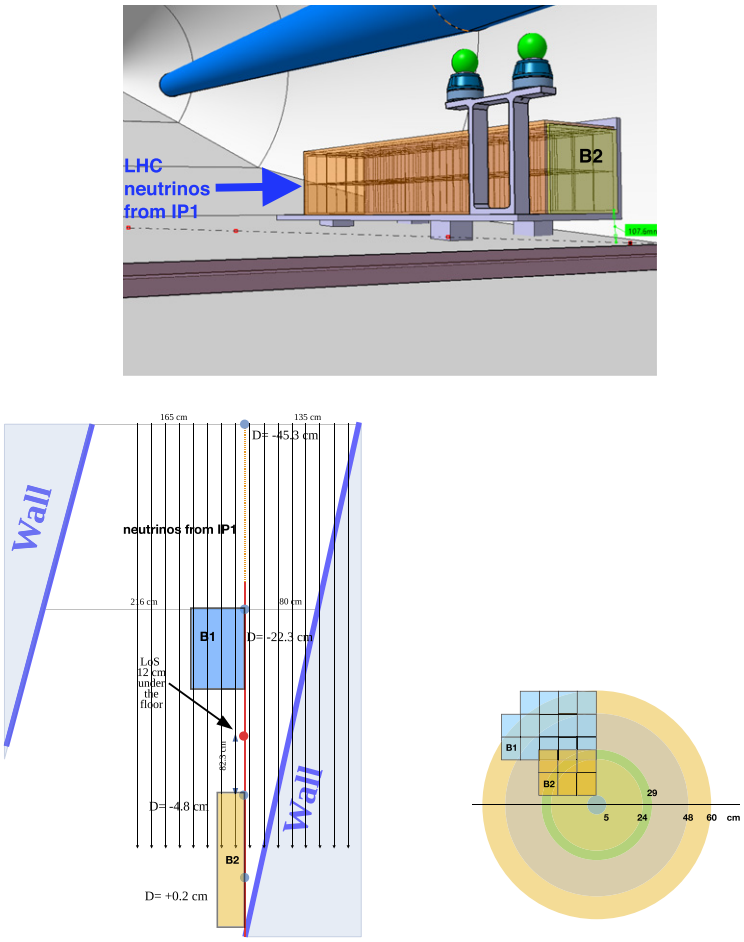

Figure 10. A possible architecture of the B2 and B1 detectors; the numbering refers to the distance to the IP: B1 is closer. Top: 3D view of B2 [12]. Bottom left: top view of B1 and B2; *D* is the height of the LoS with respect to the TI18 cavern floor, measured in different points. Bottom right: section view of B1 and B2 showing their radial distance in cm from the beam axis, which is taken as 57.6 mm above the LoS.

this physics potential is not spoiled by the flux of muon neutrinos from pion and kaon decays which is concentrated at lower energies.

4. Predicted numbers of events

In the following, we explore the neutrino event distributions in the η-energy plane, using the neutrino flux simulations of the previous section and a realistic detector design. We will consider two detectors, covering the pseudorapidity ranges, $8.0 < \eta < 9.2$ and $7.4 < \eta < 8.1$. The studies are based on large samples of simulated pp collisions: 10 million PYTHIA events of heavy hadron (c and b) production, 50 million DPMJET/FLUKA minimum bias events (extended to 400 million for the tau neutrino predictions).

A 3D view of a compact detector (B2) that subtends the pseudorapidity range $8.0 < \eta < 9.2$ is shown in figure 10 top. It consists of 108 OPERA bricks ($3 \times 2 \times 18$ bricks), it is 1.4 m long

Table 1. Neutrino CC event rate expectations for a detector configuration as shown in figure 10 for an LHC luminosity of 150 fb^{-1}. B1 (1.4 tons) and B2 (0.9 tons) acceptances subtend $7.4 < \eta < 8.1$ and $8.0 < \eta < 9.2$, respectively. Neutrino flux from c and b decays calculated with PYTHIA.

	B1	B2	B1 + B2
Integral ν fluence	4.6×10^{11}	3.4×10^{11}	0.8×10^{12}
All ν events	490	852	1342
tau flavour ν events	26	25	51
η range	7.4–8.1	8.0–9.2	
Average E_ν (RMS) GeV	700(400)	1200(600)	

and weighs 0.9 tons. The B2 detector is positioned 108 mm above the LoS: the beam axis in TI18 is centred high above the LoS by 57.6 mm, since the proton beams in IP1 cross vertically with a half-angle of 120 microradians. During fills in LHC Run 2 the beam crossing angles moved from 160 down to 120 microradians, corresponding to 76.8 mm and 57.6 mm of LoS displacement at TI18, respectively.

A second detector (B1) is placed further uphill in TI18, towards IP1. Figure 10 shows an implementation with 168 OPERA bricks: a wall of 14 bricks is replicated 12 times along the LoS. It has acceptance for $7.4 < \eta < 8.1$, it is 1.0 m long and weighs 1.4 tons. The available space in TI18 would allow for doubling B1 azimuthal acceptance and its mass.

A possible inversion from upwards to downwards of the LHC beam crossing at the ATLAS IP during Run 3 will modify the detector acceptance. It will shift to $7.7 < \eta < 8.4$ in B2 and to $7.2 < \eta < 7.8$ in B1. This slight change does not substantially modify the nature of the neutrino flux already discussed in section 3. The event rate will be reduced by ≈20%.

LHC Run 3 was extended to include 2024 and it is expected to integrate more than 150 fb^{-1} and possibly as much as 200–250 fb^{-1}. In the following, the calculated event numbers are relative to 150 fb^{-1} with upward beam crossing in IP1. In the DPMJET/FLUKA calculations, all LHC beam parameters are included. Besides the crossing angle, the longitudinal bunch size is taken into account, implying a spread in the actual collision point distribution. LHC beam transverse size, which is normally negligible, and beam divergence, although included, are observed to have no relevant impact.

An event by event weight was applied to describe the neutrino interaction probability in the detector material. The weight takes into account the νN CC interaction cross section dependence on energy and on neutrino flavour. In the interesting energy range of 10 GeV to a few TeV, a linear energy dependence for neutrino and antineutrino on nucleon inclusive CC cross sections was used, $\sigma/E_\nu = 0.677 \times 10^{-38}\,\mathrm{cm}^2\,\mathrm{GeV}^{-1}$ and $\sigma/E_{\bar{\nu}} = 0.334 \times 10^{-38}\,\mathrm{cm}^2\,\mathrm{GeV}^{-1}$, which reproduces the measured cross sections for muon and electron neutrinos up to about 300 and 100 GeV, respectively [2]. For the CC cross section of τ neutrinos on nucleons, we referred to the theoretical isoscalar calculations in reference [27]; the predictions are smaller by ≈15% than for muon neutrinos, due to the effect of the F4 and F5 structure functions [28]. In the simulation only the lead mass is assumed to contribute to the neutrino interaction probability, presenting $0.68 \times 10^{27}\,\mathrm{N\,cm}^{-2}$ in 1 m of detector thickness.

Table 1 summarizes the expected numbers and characteristics of the CC events for the detector configuration shown in figure 10 using the PYTHIA neutrino flux. The predicted energy spectra of neutrino CC events in both the B1 and B2 detectors are shown in figure 11. The spectrum is biased towards high energies, since the νN cross section grows rapidly with neutrino energy.

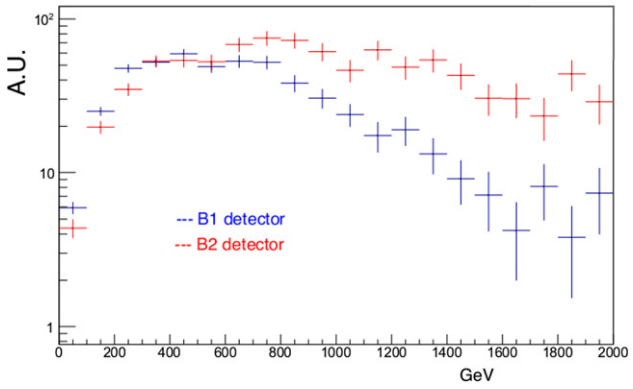

Figure 11. Predicted energy spectra of neutrino CC interactions in the B1 and B2 detectors, using the PYTHIA simulated neutrino flux.

Table 2. Expectations for neutrino CC event rate and average energy, using in input the neutrino flux calculated with the DPMJET/FLUKA event generator and the simulation of the LHC magnetic optics, for an LHC luminosity of 150 fb^{-1}. Detector B1 (1.4 tons) and B2 (0.9 tons) acceptances subtend $7.4 < \eta < 8.1$ and $8.0 < \eta < 9.2$, respectively.

	B1		B2	
	All	Exclude ν from π, K decay	All	Exclude ν from π, K decay
μ flavour ν events	929	267	1516	538
e flavour ν events	302	292	616	598
τ flavour ν events	16	16	28	28
All ν events	1247	575	2160	1164
Average E_ν (RMS) GeV				
μ flavour ν events	385(400)	535(315)	740(685)	1145(710)
e flavour ν events	560(350)		1165(715)	
τ flavour ν events	630(370)		1095(720)	

Calculation with PYTHIA accounts for the contribution from decays of heavy quarks (c and b). The additional contribution of pion and kaon decays was studied in minimum bias events generated by DPMJET generator that also included charm production. Charged pions and kaons were transported in FLUKA along the LHC straight section and through the LHC magnetic optics until they decayed. The same detector response function was used as for calculations using PYTHIA. The results are shown in table 2.

The predictions for electron and tau neutrino interaction rates using PYTHIA and DPMJET/FLUKA are in good agreement, and their spectra are consistent. The ν_e and ν_τ events in the B1 and B2 detectors probe charm production and neutrino physics in two rather independent energy bins. For muon neutrinos, PYTHIA and DPMJET compare well, when neutrinos from pion and kaon decays, which populate the lower energy part of the spectrum in DPMJET, are excluded. Figure 12 shows the energy spectra of electron and muon neutrino CC events predicted using DPMJET in the two pseudorapidity ranges under consideration.

The detailed calculations on pion and kaon transportation along the LHC optics and their decay also provide an estimate of the muon flux in TI18 (figure 13). In the region occupied

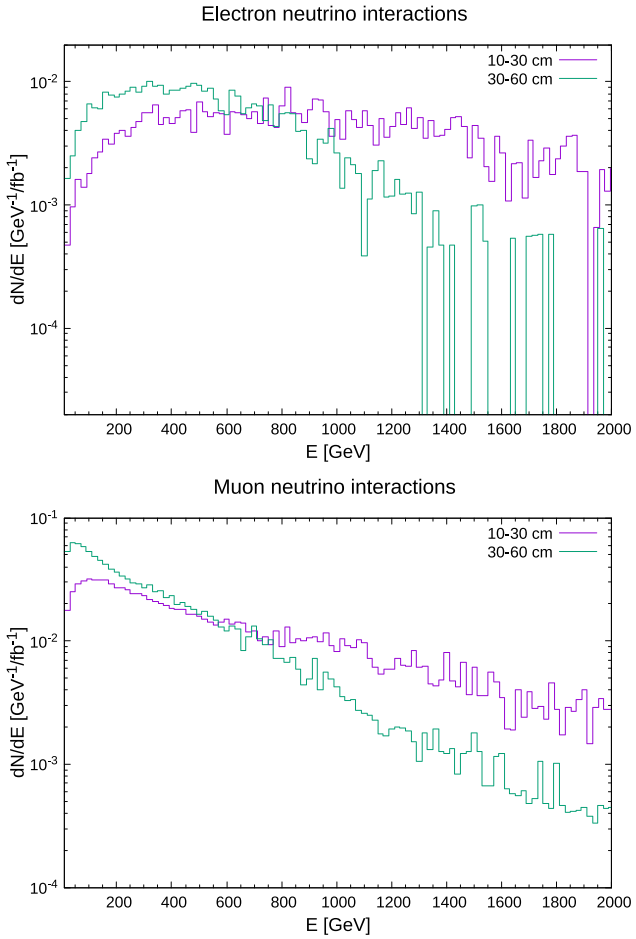

Figure 12. Predicted energy spectra of neutrino CC interactions in the B1 (30–60 cm radially out from beam axis) and B2 (10–30 cm radially out) detectors, using the DPMJET/FLUKA simulated neutrino flux.

by B1 and B2 it is expected that 10^3–10^4 muons/cm^2 in 1 fb^{-1} of LHC luminosity will be recorded: they provide an excellent tool for aligning the detector emulsion layers.

5. Summary and outlook

This work complements a previous paper [1] that discussed the physics potential of a neutrino experiment at the LHC, and identified a favorable site. The requirements were: high flux of TeV neutrinos; sizeable contribution of tau neutrinos; low machine backgrounds. It suggested that a detector could be positioned in the cavern of the TI18 (or TI12) tunnel that intercepts the LHC after the beginning of the arc, ≈480 m from the ATLAS IP. The location allows for a small size detector observing neutrinos in the $\eta > 6.7$ range.

The paper focuses on exploring the neutrino pseudorapity versus energy phase space available in TI18. The aim is to optimize the detector location and acceptance for neutrinos originating at the pp interaction point, in contrast to neutrinos from pion and kaon decays.

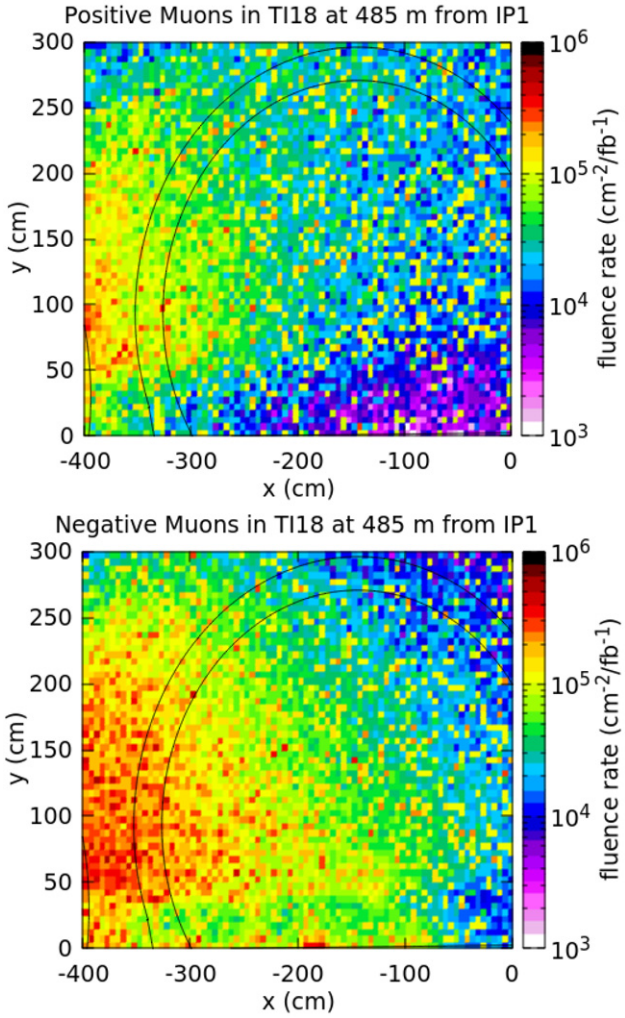

Figure 13. Muon flux in TI18 calculated with DPMJET/FLUKA and the simulation of the LHC magnetic optics. The pictures show a slice of the TI18 cavern, 485 m from IP1. The origin (0, 0) is set on the LoS. Dimensions are centimeters. The black lines delimit the tunnel wall.

Simulations of pp collisions are performed using PYTHIA [6] and DPMJET/FLUKA [7–11]. The FLUKA set-up used by the CERN EN-STI team allows for tracking charged pions and kaons along the LHC machine until they decay; the simulation includes LHC beam parameters.

It is shown that a detector position slightly off the LHC beam LoS, covering the angular acceptance $7.4 < \eta < 9.2$, is convenient for observing neutrinos originating at the IP since their distribution falls off very rapidly at larger pseudorapidities, closer to the beam LoS. The η acceptance is split into two regions, $7.4 < \eta < 8.1$ and $8.0 < \eta < 9.2$, which have slightly different kinematics constraints and neutrino flux compositions, and are independently studied. Electron neutrinos are shown to originate mainly from charm decays; their behaviour is consistent with kinematics predictions. Their flux and spectra are in excellent agreement between

PYTHIA and DPMJET, in both η ranges. Similary for neutrinos of the tau flavour, which originate in $D_s \to \tau\nu_\tau$ decays and subsequent τ decays. Muon neutrinos at high energy (0.5–1 TeV and beyond) are originating at the IP from charm and their spectrum is consistent with that of electron neutrinos, while at lower energies the muon neutrino rate is dominated by pion and kaon decays.

Rates and energy spectra are estimated of neutrino interactions in two detectors, B1 and B2, made of lead interleaved with nuclear emulsions, with masses of 1.4 tons and 0.9 tons and covering the pseudorapidity ranges $7.4 < \eta < 8.1$ and $8.0 < \eta < 9.2$. It is assumed to take data during the LHC Run 3, integrating a luminosity of 150 fb^{-1}. A few thousand high energy electron and muon neutrino CC interactions can be collected, and over 50 tau neutrino CC events. The average energies are ≈600 GeV in B1 and ≈1.1 TeV in B2 , with large RMS of ≈0.5 TeV.

The electron and muon neutrino samples can be used for constraining the theoretical uncertainties, in charm production in pp collisions, that limit the calculations of the neutrino flux. The tau neutrino sample can be used to study tagging techniques in this very boosted regimes and provides, although with limited precision, a measurement of the ν_τN cross section. This is very useful information in view of an experiment at HL–LHC to collect 3000 fb^{-1}.

Acknowledgments

We would like to thank I Ajguirey, A Ball, A Dabrowski, D Dattola, J Gall, F Gasparini, V Klyukhin, M Komatsu, S Mallows, A Perrotta, V Tioukov, W Zeuner and the CERN EN/SMM-RME group for help in various parts of our studies.

ORCID iDs

M Brucoli https://orcid.org/0000-0002-1441-0743
G M Dallavalle https://orcid.org/0000-0002-8614-0420
L Patrizii https://orcid.org/0000-0002-9712-977X

References

[1] Beni N *et al* 2019 Physics potential of an experiment using LHC neutrinos *J. Phys. G: Nucl. Part. Phys.* **46** 115008
[2] Tanabashi M *et al* (Particle Data Group) 2018 Review of particle physics *Phys. Rev.* D **98** 030001
[3] IceCube Collaboration 2017 Measurement of the multi-Tev neutrino interaction cross-section with IceCube using Earth absorption *Nature* **551** 596
[4] ALEPH, DELPHI, L3, OPAL, SLD Collaborations, LEP Electroweak Working Group, SLD Electroweak Group and SLD Heavy Flavour Group 2006 Precision electroweak measurements on the *Z* resonance *Phys. Rep.* **427** 257
[5] Ahmis Y *et al* (Heavy Flavor Averaging Group) 2017 *Eur. Phys. J.* C **77** 895
[6] Sjöstrand T *et al* 2015 An introduction to PYTHIA 8.2 *Comput. Phys. Commun.* **191** 159
[7] Bohlen T T *et al* 2014 The FLUKA code: developments and challenges for high energy and medical applications *Nucl. Data Sheets* **120** 211–4
[8] Battistoni G *et al* 2015 Overview of the FLUKA code *Ann. Nucl. Energy* **82** 10–8
[9] Roesler S, Engel R and Ranft J 2001 The Monte Carlo event generator DPMJET-III *Proc. of the Monte Carlo 2000 Conf.* (Lisbon 23–26 October 2000) ed A Kling, F Barao, M Nakagawa, L Tavora and P Vaz (Berlin: Springer) pp 1033–8
[10] Fedynitch A 2015 Cascade equations and hadronic interactions at very high energies *CERN-THESIS-2015-371* https://cds.cern.ch/record/2231593

[11] Lechner A *et al* 2019 Validation of energy deposition simulations for proton and heavy ion losses in the CERN large Hadron collider *Phys. Rev. Accel. Beams* **22** 071003
[12] Engineering drawing courtesy of CERN SMB Department.
[13] OPERA Collaboration 2015 Discovery of τ neutrino appearance in the CNGS neutrino beam with the OPERA experiment *Phys. Rev. Lett.* **115** 121802
[14] DONuT Collaboration 2008 Final tau-neutrino results from the DONuT experiment *Phys. Rev.* D **78** 052002
[15] Aoki S *et al* (The DsTau Collaboration) 2020 DsTau: study of tau neutrino production with 400 GeV protons from the CERN-SPS *J. High Energy Phys.* JHEP01(2020)033
[16] Agafonova N *et al* (OPERA Collaboration) 2012 Momentum measurement by the multiple Coulomb scattering method in the OPERA lead-emulsion target *New J. Phys.* **14** 013026
[17] Juget F(OPERA Collaboration) 2009 Electromagnetic shower reconstruction with emulsion films in the OPERA experiment *J. Phys.: Conf. Ser.* **160** 012033
[18] Shirobokov S *et al* 2018 Machine learning for electromagnetic showers reconstruction in emulsion cloud chambers *J. Phys.: Conf. Ser.* **1085** 042025
[19] Berghjaus P, Montaruli T and Ranft J 2008 Charm production in DPMJET *J. Cosmol. Astropart. Phys.* JCAP06(2008)003
[20] LHCb Collaboration 2012 Measurement of charged particle multiplicities in pp collisions at $\sqrt{s} = 7$ Tev in the forward region *Eur. Phys. J.* C **72** 1947
[21] Antchev G *et al* 2012 Measurement of the forward charged particle pseudorapidity density in pp collisions at sqrts = 7 TeV with the TOTEM experiment *Europhys. Lett.* **98** 31002
[22] Skands P, Carrazza S and Rojo J 2014 Tuning PYTHIA 8.1: the monash 2013 tune *Eur. Phys. J.* C **74** 3024
[23] De Rùjula A, Fernandez E and Gòmez-Cadenas J J 1993 Neutrino fluxes at future hadron colliders *Nucl. Phys.* B **405** 80–108
[24] Bai W, Diwan M, Garzelli M V, Jeong Y S and Reno M H 2020 Far-forward neutrinos at the large hadron collider *CERN-TH-2020-007, BNL-213623-2020-FORE* arXiv:2002.03012v1
[25] Park H 2011 The estimation of neutrino fluxes produced by proton–proton collisions at $\sqrt{s}$=14 TeV of the LHC *J. High Energy Phys.* **10** 092
[26] FASER Collaboration 2020 Detecting and studying high-energy collider neutrinos with FASER at the LHC *Eur. Phys. J.* C **80** 61
[27] Jeong Y and Reno M 2010 Tau neutrino and antineutrino cross sections *Phys. Rev.* D **82** 033010
[28] Albright C H and Jarlskog C 1975 Neutrino production of M^+ and E^+ heavy leptons (I) *Nucl. Phys.* B **84** 467